Further improvements in the structural analysis of DEMO Divertor Cassette body and design assessment according to RCC-MRx

Paolo Frosi[a], Pietro Alessandro Di Maio[b], Domenico Marzullo[c], Giuseppe Mazzone[a], Jeong-Ha You[d],

[a] *Department of Fusion and Technology for Nuclear Safety and Security, ENEA C. R. Frascati, via E. Fermi 45, 00044 Frascati (Roma), Italy*
[b] *University of Palermo, Viale delle Scienze, Edificio 6, 90128 Palermo, Italy*
[c] *CREATE Consortium/University of Naples Federico II, Department of Industrial Engineering (DII), Piazzale Tecchio 80 – 80125 Napoli, Italy*
[d] *Max Planck Institute for Plasma Physics, Boltzmann Str. 2, 85748 Garching, Germany*

This paper presents the enhancements related to the structural analyses of DEMO Divertor in the framework of the EUROfusion Power Plant Physics & Technology (PPPT) program. This activity started two years ago and its preliminary results were published in previous papers. It has been divided in some areas defined by the similarity of the matters they contain: the structural analysis, of utmost importance, has been preceded by a preliminary phase, like the geometry definition or the thermal and the electro-magnetic analysis for loads evaluation; then the structural analysis has been finally confirmed with further evaluations related to excessive deformation or plastic instability. In spite of these phases respect a logical order and they are also dependent on time, they have been started and carried on simultaneously as reported in the previous works. This paper discusses the improvements adopted either in the preliminary phases or in the main structural analysis. Specifically it highlights the introduction of the thermal and electro-magnetic loads application in terms of a detailed spatial distribution that is now available. More a detailed geometry of the supports has been introduced in the models and their thermal and structural behavior has been investigated. The structural assessment, according to the Design and Construction Rules for Mechanical Components of Nuclear Installation (RCC-MRx), has been adapted to the enhanced load evaluation.

Keywords: FEM, DEMO, Divertor, structural analysis, thermal analysis, RCC-MRx

1. Introduction

This paper summaries the last enhancements obtained in the structural design of DEMO Divertor. This activity began two years ago with provisional outcomes of the structural analysis that, in turn, was using the preparatory phases results that were obtained with some approximations. The summary of this previous activity can be found in [1-2]. The whole design activity has been improved either in the preparatory phases (e.g. neutron analysis, geometric dimensioning, thermal analysis) or in the proper stress-strain evaluation. These improvements have allowed to leave the previous hypothesis of thermal and electric-magnetic loads uniform distribution as, in the meanwhile, a punctual evaluation has become available. The choices related to the attachments have allowed to reach some fundamental points about their effects on global displacements, deformations and reaction forces. In order to understand better the whole mechanical behavior, every kind of load has been analyzed separately: so some qualitative deductions can be done by comparing the results obtained in each case (with the awareness that the component finds itself in a plastic state, they can be summed very carefully). More, as previously done, a simplified but meaningful assessment according to RCC-MRx code has been executed.

2. Preparatory phase

This step is related to the introductory work aimed to prepare all the input data needed to perform the proper structural analysis.

The new geometry of the Divertor Cassette has been the first supplying: its development has been described adequately in [3]. A complete image of the new geometry has reported in fig. 1.

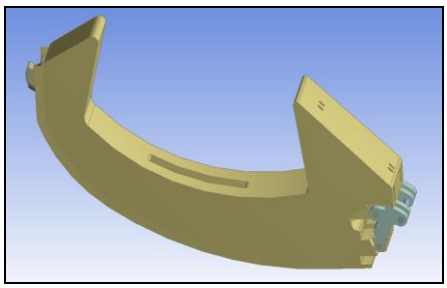

Fig. 1: 2016 CAD model of the Cassette Divertor

Neglecting all details that have been explained in [3], in comparison with the previous geometry [4], it is trustworthy for the following to highlight the change of poloidal and toroidal internal ribs thickness from 30 to 20 mm, while the external cassette plates remain 30 mm thick. The main improvements has regarded the internal structure to optimize the cooling paths and the cassette strength.

The nuclear heating are the main set of data needed either for thermal or structural analysis. They have been evaluated with a detailed subdivision of the Divertor volume: the thermal power has been listed for each cell the Cassette Divertor has been divided in, and it is going to be published [5].

This set of data has been adopted for the coupled–field thermofluid dynamic analysis reported in [6].

Corresponding author's email: paolo.frosi@enea.it

Unlike from the previous works [1-2], the thermal power hasn't been applied uniformly: and it has been possible to simulate the temperature gradients in a more realistic manner (and more useful for the structural analysis purposes): in fig. 2 there is the obtained temperature contour plot.

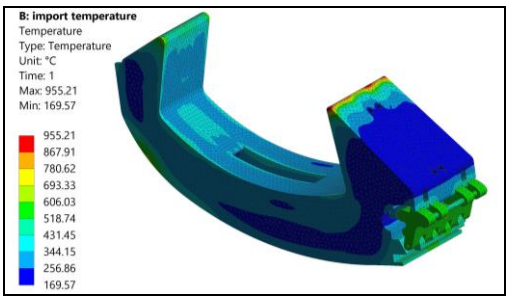

Fig. 2: temperature contour plot

The region at the top of the outer vertical targets that exhibits high temperatures can be neglected for a global structural analysis and it can be overcome with a more suitable geometric choice as stated in [6].

The same concept must be repeated for the electric-magnetic forces whose detailed distribution for the whole DEMO tokamak has been evaluated with another study [7]. Neglecting all details, the total forces acting on the Cassette Divertor have been reported in fig. 3 during the time interval across the disruption event (in this case downward major disruption) with clear symbolism of the directions they relate to. The radial direction is considered positive in the outward way, the vertical one is positive upward and the positive toroidal direction follows the cartesian reference right-hand rule.

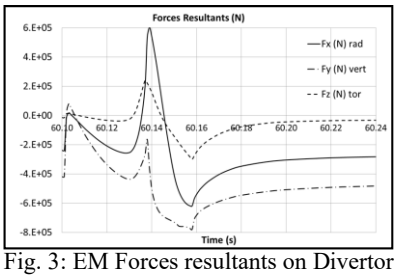

Fig. 3: EM Forces resultants on Divertor

3. Loads acting separately

These sets of input data allow to study the state of stress caused independently from one another. As obtained previously [1-2], the thermal loads play a relevant role: indeed in the fig.4 there is the contour plot when the Cassette has been fixed in the inner region (Nose constrained) and in the outer position (external knuckle pin fixed on the vacuum vessel).

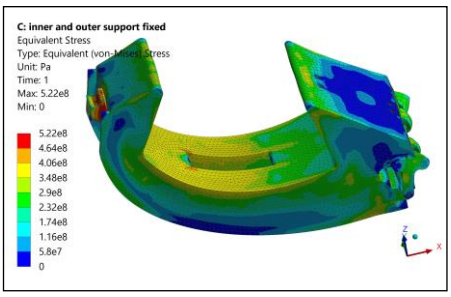

Fig. 4: Equivalent stresses due to thermal loads

The highest stresses are on the Nose and this fact suggests to enlarge this attachment to spread the reaction forces over a wider region; in the knuckle region the plastic strain are about 10%: this fact will be more emphasized in the following cases and it is due to the overall deformation of the Cassette: in the fig. 5 there is the vertical displacement contour plot: it can be seen that the central zone goes downward while the outer zone goes upwards (the inner zone is practically fixed due to the Nose great stiffness).

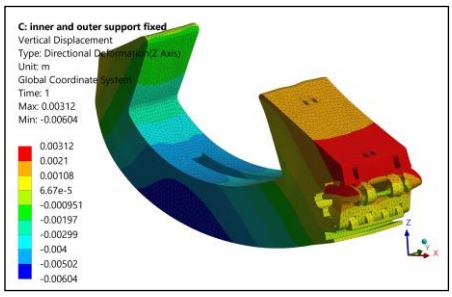

Fig. 5: vertical displacements due to thermal loads

The knuckle hinges have been thought for the installation but in doing so they suffer too much plastic strain during operation. This behavior can be predicted because now the thermal loads haven't been applied uniformly; the material near the Dome region is hotter than that one of the bottom side and its greater lengthening can only result in an increase of curvature because the position of the attachments doesn't allow to straighten to the same upper central region. This finding is different from what stated previously. More in fig. 6 there is the radial displacement contour plot: in the outer region a "butterfly distribution" can be seen: it is a further proof of the aforementioned curvature increase.

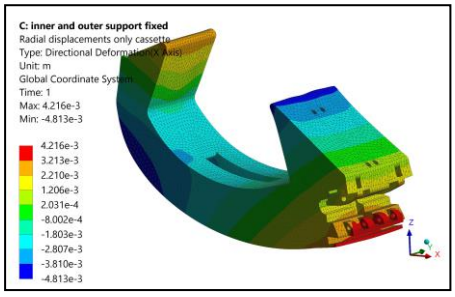

Fig. 6: radial displacements due to thermal loads

For what concern the electro-magnetic loads, according to the fig. 3, two analysis have been done: one relative to the positive maximum (t = 60.139 s) and one to the negative maximum (t = 60.158 s). The import of the forces into the structural model considers surely the spatial distribution of the magnetic force density, but there is a great difference on mesh density (one related to the whole tokamak and one related only to a component), so the resultants in each direction (radial, vertical and toroidal) aren't preserved exactly during importation. The case more interesting (that is with the higher equivalent stresses) is the one at t = 60.139s (positive maximum): its equivalent stress contour plot is reported in fig. 7. Also in this case the Knuckle is subjected to high distortions while the cassette doesn't suffer plastic strain except in the housing of the knuckle pins.

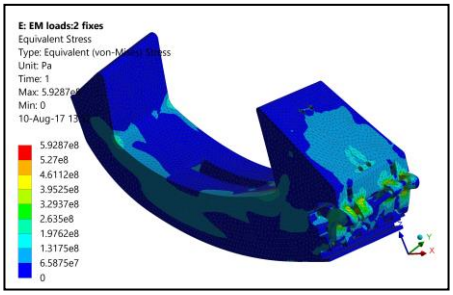

Fig. 7: equivalent stresses due to magnetic forces

The cooling water pressure has been the last load case studied. The last adopted values for the water are [6]: 3.5 MPa and 180°C for the inlet pressure and temperature respectively. In the fig. 8 there is the equivalent stress contour plot related to this case: now in the supports and in the cassette there aren't any plastic strain. The state of stress is globally low even though it's a little higher than that found previously due to the decreased thickness of the internal ribs.

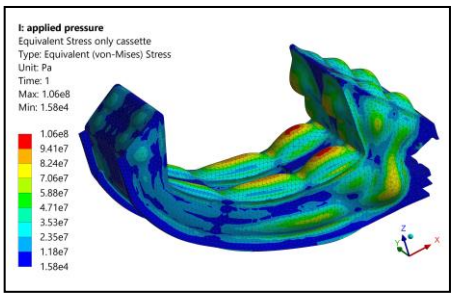

Fig. 8: equivalent stresses due to applied pressure

4. Loads acting together

All the cases examined above are useful to understand the complete behavior of the Cassette when they acting together. It is possible to identify 3 main cases worth to be analyzed:

1) Electric-magnetic and thermal loads
2) Pressure and thermal loads
3) Pressure, electric-magnetic and thermal loads.

The first case shows again that the thermal loads play a greater role than the EM forces: indeed the whole behavior of the cassette resembles more to the case of the thermal loads than that of the EM forces. In the fig. 9 there is the related equivalent stress contour plot:

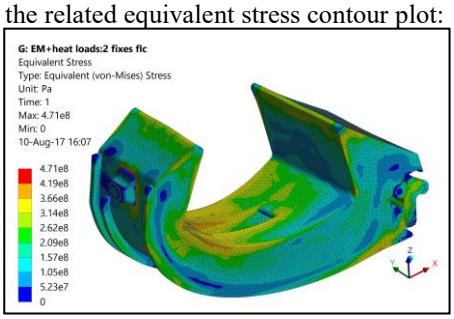

Fig. 9: equivalent stresses due to thermal and EM loads

The highest level of stress is located in the sharp corners of the central hole that can be overcome improving locally the geometry and refining the mesh and, more, behind the Nose. As further proof that this case is dominated by thermal loads, in the fig. 10 there is the radial displacements of the cassette that is very similar to that reported in fig. 6 when thermal loads act alone. So the same considerations made above can be repeated here. More the knuckle pins exhibit high plastic strain that confirms the necessity to review their geometry.

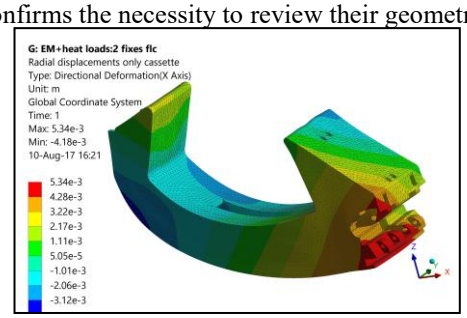

Fig. 10: radial displacement due to thermal and EM loads

It must be noted that when only the thermal loads act, the radial reactions are equal and opposite (inboard reaction is directed outward and outboard reaction is directed inward), just like the vertical reactions that are directed downward (for the Nose) and upward (for the Knuckle); when the EM forces are superimposed it results a decrease of the absolute values (given by the EM forces resultant) of the inboard reactions while the outboard reaction values remain the same. Indeed the Nose in fig.9 has not any more the highest values like in fig. 4. The reaction forces due to thermal loads (about 6 MN) are one order of magnitude greater than that due to EM forces (570 kN). This is an implicit verification of the correctness of the analysis procedure and it is useful to study in the future a way to limit the radial action of the Cassette on the Vacuum Vessel.

The second case, regarding the pressure and thermal loads, can be put in the same frame of the previous ones. In fig. 11 is reported the equivalent stress contour plot (similar to fig. 4); also the Cassette radial displacement in this case is similar to what obtained in fig.6 and it isn't reported.

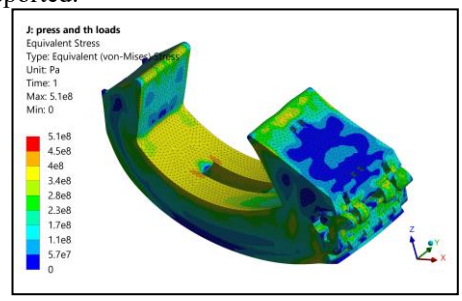

Fig. 11: equivalent stresses due to thermal and pressure loads

The knuckle pins suffer again high plastic strain as reported in fig. 12 (pin connected to the Cassette).

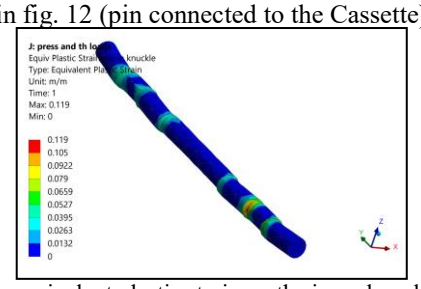

Fig. 12: equivalent plastic strain on the inner knuckle pin

The last case doesn't add any further information to what already stated because the pressure loads influence a little the global behavior of the Cassette. In fig. 13 there is the equivalent stress related to this case.

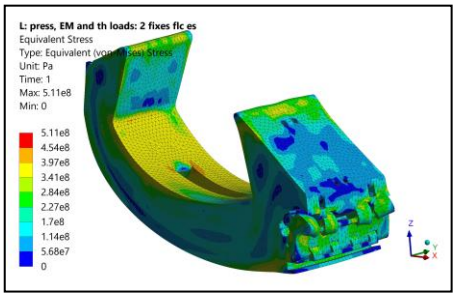

Fig. 13: equivalent stresses caused by all loads

In these two last cases the highest values are located in the region where the Nose is attached to the Cassette (not shown) unlike the first case where the EM forces had reduced the total action on the inner support. Now the pressure action prevails and the radial reaction forces shown by the supports are increased resulting in higher equivalent stress in that region. As last confirmation of the coherence of the whole analysis it is reported in fig. 14 the radial displacement of the knuckle related to this case.

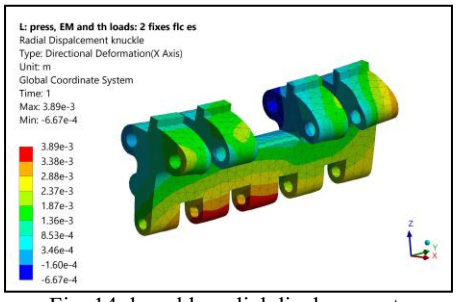

Fig. 14: knuckle radial displacements

The cinematic behavior of the knuckle is the same discussed in section 2: the outer part of the Cassette due to the prevented radial lengthening tends to go upwards (curvature increase in the Cassette central zone) and the knuckle bottom hinge exhibits a radial outward displacement giving great distortions of the whole component. This fact is also found in the Cassette in the holes for the pins that are always resulted highly stressed.

5. RCC-MRx simplified assessment

A simplified evaluation according the RCC-MRx code (level A criteria) [8] has been performed. This verification is only illustrative because fatigue and buckling were not analyzed and, in line with the adopted hypothesis, it deals with the prevention from excessive deformation and racheting: nevertheless it shows how much the operative loads result far from the limit values. The aforementioned French nuclear code typically deals with the primary stresses (membrane P_m and bending P_b) and with the line supporting segments. The primary stresses are a linearization of the stresses (along the properly defined line supporting segments) that equilibrate directly the applied loads. The line supporting segments positions have been reported in fig. 15. The assessment has been performed only for un-irradiated conditions for the same reasons reported in [1-2].

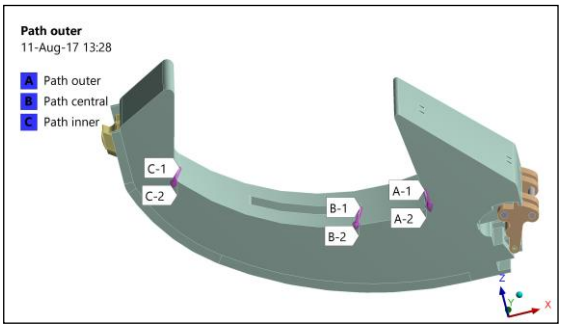

Fig. 15: line supporting segment positions

This set of analysis has been executed adopting a linear elastic material properties. The first step is made to prevent type P damages (RCC-MRx Level A criteria): that is to verify that primary stresses due to mechanical loads (water pressure) at their operation temperature are below the admissible stresses at the same temperature. Denoting with θ_m the mean temperature along the path and with S_m is the maximum allowable stress (temperature dependent values that are reported inside the code), the classical two relations for the three paths have been verified:

$$\overline{P_m} \le S_m(\vartheta_m) \tag{1}$$

$$\overline{P_m + P_b} \le 1.5 \cdot S_m(\theta_m) \tag{2}$$

where P_m is the general primary membrane stress intensity, P_m+P_b is primary membrane plus bending stress intensity: in table 1 there is the result of this step.

Table 1. Verification against type P damages (values in MPa).

Path outer		θ_m = 249°C
P_m = 13.3	S_m = 199	
P_m+P_b = 19.5	1.5* S_m = 299	
Path central		θ_m = 283°C
P_m = 5.5	S_m = 194	
P_m+P_b = 13.2	1.5* S_m = 292	
Path inner		θ_m = 326°C
P_m = 5.8	S_m = 187	
P_m+P_b = 7.3	1.5* S_m = 281	

The second step is related to the stress range evaluation ($3S_m$ rule) that is the state of stress due to the full action of nuclear heating minus the state of stress due to stand-by condition (the component at the same temperature of bulk water) always written as ΔQ. This fact can be summarized by the relation:

$$Max\overline{(P_l + P_b)} + \overline{\Delta Q} \le 3 \cdot S_m \tag{3}$$

The first term of this relation is the same of the previous analysis. With the same symbolism used in (3), in the tab. 2 the essential results have been reported.

Table 2. Verification against type S damages (values in MPa).

Path outer	
Max(P_m+P_b)+ΔQ = 157	3* S_m = 597
Path central	
Max(P_m+P_b)+ΔQ = 186	3* S_m = 583
Path inner	
Max(P_m+P_b)+ΔQ = 514	3* S_m = 562

At least for this simplified analysis, the two steps of the RCC-MRx assessment can be considered fully verified.

6. Conclusions

A complete and detailed elastic-plastic analysis has been performed for the Demo Divertor Cassette. The uniform application of thermal and magnetic loads has been overcome: the actual punctual distribution has allowed to know better the cinematic behavior of the Divertor Cassette. It is found once again that the thermal loads exhibit the greater influence on the component (in this case the support reactions are 10 times higher than that caused by electric-magnetic loads); so it tends to lengthen itself and to increase its curvature (as stated above). This determines a high state of stress for the Nose and high plastic strains for the Knuckle, its pins and the pin housing on the Cassette. The outboard region of the Cassette shows a sort of rotation with radial outward and vertical upward displacements. This fact suggests to review the knuckle geometry and the pins positions in order to accomplish such field of displacements.

Acknowledgments

This work has been carried out within the framework of the EUROfusion Consortium and has received funding from the Euratom research programme 2014-2018. The views and opinions expressed herein do not necessarily reflect those of the European Commission.

The computing resources and the related technical support used for this work have been provided by CRESCO/ENEAGRID High PerformanceComputing infrastructure. It is funded by ENEA, the Italian National Agency for New Technologies, Energy and Sustainable Economic Development and by Italian and European research programs, see http://www.cresco.enea.it/english for information

References

[1] P. Frosi, G. Mazzone, J. You, Structural design of DEMO Divertor Cassette Body: provisional FEM analysis and introductive application of RCC-MRx design rule, Fusion Engineering and Design, 109-111 (2016) 47-51

[2] P. Frosi, C. Bachmann et al., Structural analysis of DEMO Divertor Cassette Body and design study based on RCC-MRx, Fusion Engineering and Design, (2017) article in press

[3] EFDA_D_2MZ59L, G. Di Gironimo, Development of the CAD model of the Divertor system

[4] EFDA_D_2M5EEF, G. Di Gironimo, CAD Model of the Divertor CB system 2015

[5] R.Villari, Private communication

[6] P. A. Di Maio, S. Garitta, J. H. You, G. Mazzone, E. Vallone, M. Marino, Computational thermofluid-dynamic analysis of DEMO divertor cassette body cooling circuit, this conference.

[7] EFDA_D_2NAZYR, M. Roccella, EM DGM including TFCs and EM analyses of Plasma disruptions plus TFCs FD

[8] RCC-MRx 2012 AFCEN Edition, Design and Construction Rules for Mechanical Components of Nuclear Installation